

We sincerely thank the Referee for the valuable comments. Our manuscript has been revised according to the comments from the Referee and our responses to the comments are as follows. For clarity, **the comments** are reproduced **in blue**, authors' responses are in black and **changes** in the manuscript are **in red**.

5

Responses to Anonymous Referee #3

Overview:

The manuscript by Yang et al. examined the effect of SO₂ and NH₃ on the formation of

10 SOA from 1,2,4-trimethylbenzene photooxidation. After the injection of SO₂ and/or NH₃, the apparent yield of the SOA increased after wall loss correction, which demonstrated the synergistic effect of SO₂ and NH₃ in facilitating SOA formation. The authors also used ATR-FTIR, IC, and UPLC-MS to systematically analyze the particle phase composition and identified various inorganic and organo-sulfates compounds.

15 My main comments are about the control experiment setup in this manuscript, which are discussed below. Other than the main comments, the manuscript is written clearly and comprehensive.

Major Comments:

The authors demonstrate that the addition of SO₂ and/or NH₃ during the photo-oxidation

20 experiments can enhance the SOA formation and yield. However, part of the aerosol growth can arise from the formation of H₂SO₄ or (NH₄)₂SO₄ particles even without the presence of any SOA, which should be deducted from the enhancement effect of SO₂ and/or NH₃. I suggest the authors add in three control experiments (pure SO₂, pure NH₃, and SO₂+NH₃ mixtures but with similar levels of OH radicals and UV intensity using 25 H₂O₂ or other OH generators) without any VOCs to rule out the formation of inorganic species contributing to the SOA.

Author Reply:

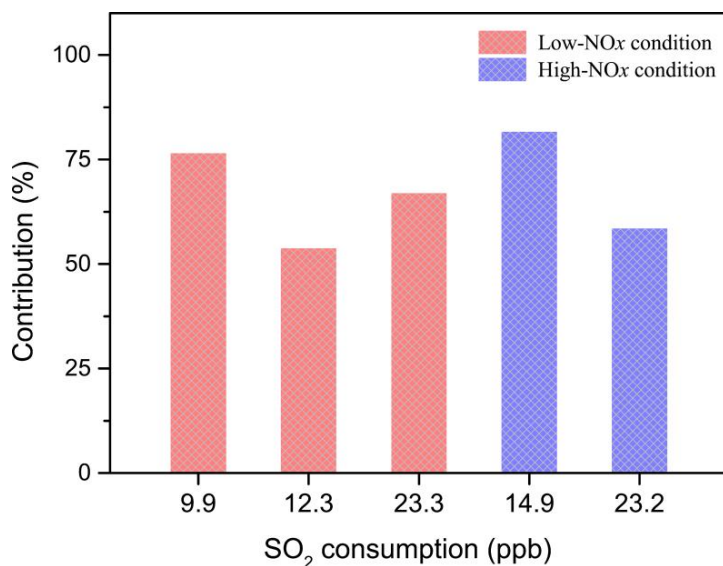
In the SO₂-added experiments, H₂SO₄ can be produced by OH oxidation of SO₂ upon photooxidation. With the coexistence of SO₂ and NH₃, the formed H₂SO₄ can be

30 neutralized by NH_3 to form $(\text{NH}_3)_4\text{SO}_4$ particles. Therefore, the addition of SO_2 and/or NH_3 to the TMB/ NO_x mixtures can lead to the increase in the volume concentration of aerosol particles by the formation of inorganic species and/or the enhanced organic products (Ye et al., 2018; Jaoui et al., 2008; Liu et al., 2019). In the present study, we discussed the SO_2 dependence of the SOA yield as shown in Fig. 4, and we showed the 35 role of NH_3 in the total particle number and volume concentrations (as discussed in Sect. 3.2.1). We believe that the introduction of SO_2 can enhance SOA yield based on our careful analysis as following:

(1) Some studies on the effects of SO_2 and/or NH_3 on SOA formation employed aerosol mass spectrometer to measure in-situ the inorganic and organic components in 40 aerosol particles (Liu et al., 2016; Chen et al., 2019). For our online measurement of aerosol particles, we solely used SMPS, whose data are insufficient to quantitatively explain the contribution of organic aerosols to the increase in aerosol mass. Offline measurement methods are also commonly adopted in chamber studies. Ion chromatography (IC) is one of the most widely used instruments providing inorganic 45 aerosol information. Kleindienst et al. (2006) investigated the SO_2 effects on SOA yields from the isoprene/ NO_x / SO_2 photooxidation and used IC to determine the mass concentrations of inorganic components. Jiang et al. (2020) revealed the influences of SO_2 and NH_3 on furan SOA yield based on SMPS and IC measurements. In this work, the concentrations of inorganic ions were measured through IC. To determine the net 50 SOA yield, the mass of inorganic components was subtracted from the total particle mass based on IC and SMPS data as mentioned in Sect. 3.1.2 in the original manuscript (Jiang et al., 2020). When SO_2 initial levels increased from 0 to 200 ppb, the net SOA yield increased from 3.8% to 17.6% in the low- NO_x regime. Similarly, elevating SO_2 initial concentration to 228 ppb under high- NO_x condition enhanced the net SOA yield 55 by a factor of 3.49. The promoting effects of SO_2 on SOA yields were in line with previous studies (Chen et al., 2019; Liu et al., 2019).

(2) We used an estimation method to explore the contribution of the generated H_2SO_4 to the particle formation enhancement in TMB/ NO_x / SO_2 photooxidation, where

we assumed the full conversion of the consumed SO_2 into H_2SO_4 aerosol particles (Ye et al., 2018; Wyche et al., 2009). As shown in Fig. R1, the contribution of the formed H_2SO_4 to the increase in particle volume concentration was less than 100%. Furthermore, a previous study showed that half of the reacted SO_2 could transform into sulfur-containing organic species during the photooxidation of 1,3,5-trimethylbenzene/o-xylene/octane/toluene (Vivanco et al., 2011). HRMS measurements reveal the OSs production in this work, which may result in the decrease in the amount of H_2SO_4 in particle phase. Therefore, the enhanced SOA formation is also responsible for the increased particle volume concentration in the presence of SO_2 .



70 **Figure R1.** Contribution (%) of the formed H_2SO_4 to the increase in particle volume concentration during low- NO_x and high- NO_x experiments.

(3) We also performed different experiments without introducing TMB, which could provide significant information about secondary inorganic aerosol formation as suggested by the Referee. In TMB/ NO_x/SO_2 photooxidation, the consumption of 9.9 and 23.3 ppb SO_2 can cause the particle volume concentration to increase by 32.9 and 89.2 $\mu\text{m}^3 \text{cm}^{-3}$, respectively. In pure SO_2 photooxidation, the volume concentrations of the formed particles were only 25.3 and 43.2 $\mu\text{m}^3 \text{cm}^{-3}$ when the consumptions of SO_2 were 9.5 and 24.2 ppb, respectively. Comparison of the results of TMB/ NO_x/SO_2 and

pure SO₂ oxidation experiments demonstrates that the enhancement in aerosol particles
80 by SO₂ introduction cannot be solely attributed to inorganic aerosol formation.

The yields shown in Table 1, obtained after ruling out the influences of inorganic species, were net SOA yields. Now, the following note was included in Table 1 in the revised manuscript. For SOA mass calculation, the inorganic mass concentration has been subtracted from the particle mass concentration.

85

Besides, we have added the following text in the revised manuscript and supplement to provide more evidence about SO₂ effects on the net SOA yield.

Page 14, lines 401–407 in the main manuscript

We assumed full conversion of the consumed SO₂ into H₂SO₄ aerosol particles and
90 found that the contribution of the formed H₂SO₄ to the increase in particle volume concentration was less than 100% (See Sect. S2). In addition, pure SO₂ oxidation experiments without TMB addition also indicated that the enhancement in aerosol particles by SO₂ introduction cannot be solely attributed to inorganic aerosol formation (See Sect. S2). To calculate the net SOA yield, the inorganic mass concentration was
95 subtracted from the particle mass concentration based on IC measurements of generated particles.

Supplement

S2. The formed H₂SO₄ estimation and inorganic mixture experiments

In order to evaluate the SO₂ effects on SOA formation, we used the method of Ye
100 et al. (2018) to calculate the contribution of the generated H₂SO₄ to the particle formation enhancement in TMB/NO_x/SO₂ photooxidation (Ye et al., 2018; Wyche et al., 2009), where we assumed full conversion of the consumed SO₂ into H₂SO₄ aerosol particles. The contribution of the formed H₂SO₄ to the increase in particle volume concentration was less than 100% (Fig. S6), demonstrating that the enhanced SOA formation is also responsible for the increased particle volume concentration.
105 Additionally, a previous study has shown that half of the reacted SO₂ can transform into sulfur-containing organic species during the photooxidation of 1,3,5-

trimethylbenzene/o-xylene/octane/toluene (Vivanco et al., 2011). HRMS measurements revealed the OSs production in this work, which may result in the decrease in the amount of H_2SO_4 in the particle phase. Therefore, the enhancement in aerosol particles by SO_2 introduction cannot be solely attributed to inorganic aerosol formation. Pure SO_2 oxidation experiments without introducing TMB were also carried out. In the TMB/ NO_x / SO_2 regime, the consumption of 9.9 and 23.3 ppb SO_2 could cause the particle volume concentration to increase by 32.9 and $89.2 \mu\text{m}^3 \text{cm}^{-3}$, respectively. However, in pure SO_2 oxidation experiments, the volume concentrations of the formed particles were only 25.3 and $43.2 \mu\text{m}^3 \text{cm}^{-3}$ when the consumptions of SO_2 were 9.5 and 24.2 ppb, respectively. Comparison of the results of TMB/ NO_x / SO_2 and pure SO_2 oxidation experiments demonstrates that the enhancement in aerosol particles by SO_2 introduction cannot be solely attributed to inorganic aerosol formation.

120

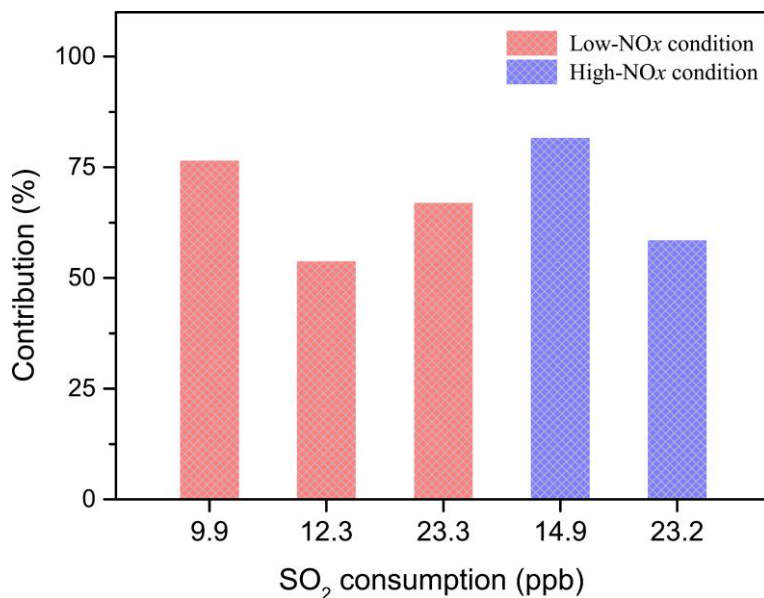


Figure S6. Contribution (%) of the formed H_2SO_4 to the increased particle volume concentration during low- NO_x and high- NO_x experiments.

125 Figure S7 shows the mass spectra with and without SO_2 and/or NH_3 are similar, suggesting that maybe inorganic species formed with OH are the likely source of enhancement. It would be important to understand that after ruling out this part of the

inorganic aerosol formation, how much enhancement the SO₂ and/or NH₃ would add to the yield of the SOA.

130 **Author Reply:**

It should be noted that Fig. S7 (now labeled as Fig. S10 in the revised supplement) compared the mass spectra of aerosol particles from NH₃-free and NH₃-added experiments. First, we carried out pure NH₃ oxidation experiments and found that aerosol particles were not formed within 480 min of UV irradiation. In addition, the 135 promoting effect of NH₃ on SOA formation was not as strong as that of SO₂ with similar level. Under SO₂-free condition, the net SOA yield increased slightly from 3.5% to 5.1% as NH₃ initial level increased from 0 to 200 ppb. Our result is consistent with the finding of Chen et al. (2020a), who showed that NH₃ did not significantly affect SOA formation from toluene/NO_x photooxidation under dry condition. Therefore, the NH₃-induced 140 changes in the absolute concentrations of organic components might be small in SO₂-free experiments, leading to similar mass spectra for Fig. S10(a) and Fig. S10(b). Under SO₂-involved conditions, the introduction of NH₃ resulted in MS differences in the range of *m/z* 200–400 as presented in Fig. S10(d). The sum of the ion signals in the ranges of 20–199, 200–299, 300–399, and 400–750 were compared in Fig. S11, where 145 it can be seen that the abundance of organic compounds with *m/z* > 200 were enhanced with the addition of NH₃ in TMB/NO_x/SO₂ photooxidation.

We have revised the text to explain why the mass spectra of aerosol particles from NH₃-free and NH₃-added experiments are similar.

Page 22, lines 640–645

150 As shown in the MS spectra of aerosol samples (Fig. S10), under SO₂-free condition, the presence of NH₃ did not result in considerable changes in peak numbers and abundance for both positive ion mode and negative ion mode. NH₃ could slightly enhance SOA formation in SO₂-free experiment as mentioned in Sect. 3.2.1. Therefore, the NH₃-induced changes in the absolute concentrations of organic components might 155 be small in SO₂-free experiments, leading to similar mass spectra for Fig. S10(a) and Fig. S10(b). In addition, the major products (Table S4) are likely generated by similar

chemical mechanisms (Fig. 8), which are not sensitive to the change in initial NH₃ levels under current experimental conditions.

It is also necessary to show how much enhancement NH₃ would add to the net SOA yield according to the Referee's suggestion. Hence, the following discussions were added in the revised manuscript.

Page 20, lines 565–576

However, the effect of NH₃ on particle formation was not as pronounced as that of SO₂ with similar concentration (Fig. 7). In TMB/NO_x/NH₃ photooxidation, the net SOA yield increased slightly from 3.5% to 5.1% as NH₃ initial level increased from 0 to 200 ppb (Table 1). Our result is consistent with the finding of Chen et al. (2020a), who showed that NH₃ did not significantly affect SOA formation from toluene/NO_x photooxidation under dry condition. Interestingly, SMPS measurements demonstrated that the coexistence of SO₂ and NH₃ can considerably promote secondary aerosol formation (Fig. 7). After subtracting the inorganic components, it was seen that the net SOA yield could increase to 13.7% with the introduction of 200 ppb NH₃ and 234 ppb SO₂, indicating the synergetic effects of NH₃ and SO₂ (Chu et al., 2016).

Another comment I have is that the enhancement of the SOA from the addition of SO₂ and/or NH₃ can also be attributed to the increase of the surface area from the formation of inorganic species, which shifts the gas-particle equilibrium more to the particle side. Can the authors discuss more about the effect of this shift of equilibrium? It seems Figure 4 shows that the first three experiments after adding SO₂ seem to follow this rule.

Author Reply:

An important mechanism of SOA formation and growth is gas-particle partitioning of semi-volatile compounds (SVOCs) generated from the atmospheric oxidation of VOCs. The gas-particle partitioning of SVOCs have a great sensitivity to particle surface areas in the batch-mode chamber experiments (Zhang et al., 2015; Han et al., 2019). Increasing particle surface area can limit the gas-wall interactions of organic vapors and is favorable for moving more SVOCs from the gas phase to the particle side

(Han et al., 2019). These additional SVOCs may undergo further particle chemistry to strongly enhance aerosol particle formation (Apsokardu and Johnston, 2018).

Recently, the effects of the particle surface area concentration on organic aerosol formation have been explored by Han et al. (2019), who found that increasing the 190 particle surface area concentrations can significantly increase organic aerosol mass yield due to greater partitioning of semi-volatility organic products to the particle-phase. In addition, some studies have confirmed that the SOA yields depend on the surface areas of inorganic aerosols when condensation of organic vapors onto particles is kinetically limited (McVay et al., 2014; Nah et al., 2016; Zhang et al., 2014). In the 195 present work, the surface area concentrations of aerosol particles increased with increasing mixing ratios of SO_2 and/or NH_3 inside the chamber (Table 1), which may facilitate the gas-particle equilibrium shifting to the particle phase. The particle surface area concentrations have been included in Table 1. Based on the suggestion of the Referee, we have enriched the discussion in the revised manuscript as following:

200 **3.1.2 SOA yield in SO_2 -added photooxidation**

Page 14, lines 422–438

In addition, the particle surface area concentrations significantly increased with increasing SO_2 initial concentrations in both low- NO_x and high- NO_x conditions (Table 1), which might also result in the enhancement in the SOA yield. Besides gas-particle 205 partitioning of SVOCs, the fate of SVOCs in the chamber also include chemical reactions and chamber wall losses. Therefore, in the batch-mode chamber experiments, the gas-particle partitioning of SVOCs have a great sensitivity to particle surface areas (Zhang et al., 2015; Han et al., 2019). Recently, Zhao et al. (2018) examined the SO_2 effects on the SOA formation and suggested that providing additional particle surfaces 210 by SO_2 -induced new particle formation leads to the increase in SOA yield. The effects of the particle surface area concentration on organic aerosol formation were explored by Han et al. (2019), who also found that increasing the particle surface area concentrations can significantly increase the organic aerosol mass yield due to greater partitioning of semi-volatility organic products to the particle-phase. Increasing the

215 particle surface area can limit the gas-wall interactions of organic vapors and is favorable for the movement of more SVOCs from the gas phase to the particle side (Han et al., 2019). These additional SVOCs can also undergo further particle chemistry such as acid-catalyzed heterogenous reactions to strongly enhance aerosol particle formation in TMB/NO_x/SO₂ photooxidation (Apsokardu and Johnston, 2018).

220 **3.2.1 Particle formation and growth in NH₃-involved photooxidation**

Page 20, lines 576–580

225 The flux of the gas-phase products diffusing to a particle partly depends on the surface area of the particle. The coexistence of SO₂ and NH₃ promoted the increase in particle surface area concentrations (Table 1). The ability of particle formation originating from gas-to-particle conversion may be significantly stronger with SO₂ and NH₃ introduction, leading to the enhancement in particle formation.

3.2.2 Particle chemical composition in NH₃-involved photooxidation

Page 23, lines 665–668

230 The introduction of SO₂ and NH₃ lead to the formation of ammonium sulfate (Fig. S12), which is an attractive condensation sink for organic vapors. High particle surface area concentration in TMB/NO_x/SO₂/NH₃ experiments may increase the abundance of organic compounds in the bulk phase.

Minor Comment:

235 L217: Can the author make an additional plot in the SI or show how the size dependent wall loss factor is generated?

Author Reply:

240 The wall-loss of particles are commonly evaluated by seed-only experiments where inert ammonium sulfate (AS) particles are used (Chen et al., 2019; Charan et al., 2020). In the current work, the AS solution was added to a TSI atomizer (Model 3076) to produce droplets, which passed simultaneously through a silica gel diffusion dryer to inject dry AS particles into the chamber. AS particles were lost to the chamber walls due to diffusion, gravitational settling, and electrostatic forces during experiment and

the mass size distributions of AS particles were measured by SMPS for 480 min.

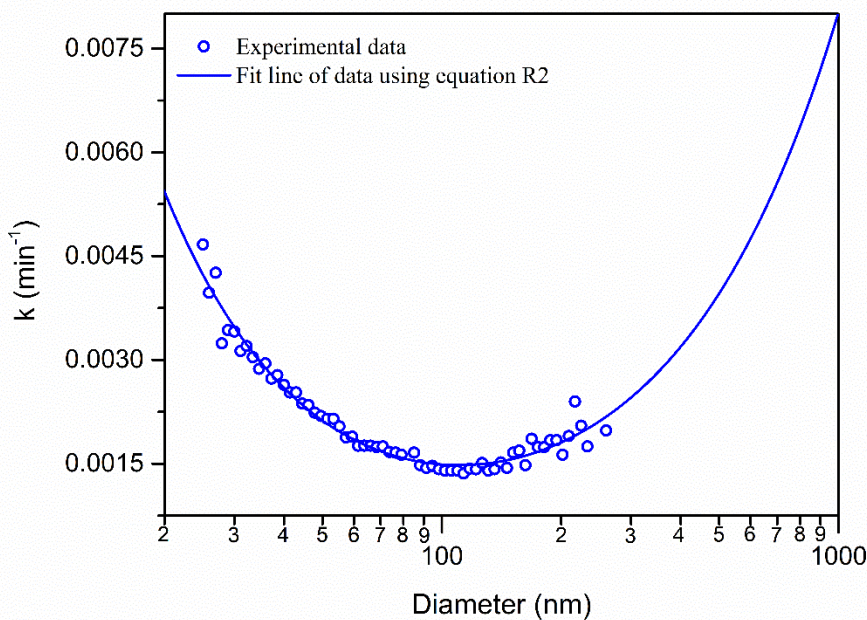
245 The size-dependent particle wall-loss rate constants were determined based on the SMPS-measured particle size distribution. First-order loss rate constants (k_i) of particles in each size bin i across all measured sizes were firstly calculated as the slope of the corresponding ln-linear fit line:

$$\ln[M_i(t)] = -k_i t + C \quad (\text{R1})$$

250 where M_i ($\mu\text{g m}^{-3}$) is the mass concentration of particles in the size bin i at time t (min) and C is an arbitrary constant. Then, the relationship between the k_i and the particle diameter ($d_{p,i}$) can be described as follows:

$$k_i(d_{p,i}) = ad_{p,i}^b + cd_{p,i}^{-d} \quad (\text{R2})$$

The optimized fitted line shown in Fig. R2 can express well our independent seed experimental results.



255 **Figure R2.** Wall loss rate constant of particles as a function of particle diameter.

The description about the wall loss experiments has been updated in the revised manuscript as follows:

260 In order to determine the particles wall loss rates, we carried out independent wall loss experiments. An aqueous solution of ammonium sulfate was fed to a constant output

atomizer (Model 3706, TSI, USA) to produce droplets, which passed simultaneously through a silica gel diffusion dryer to introduce dry particles into the chamber. The size distributions of ammonium sulfate particles were measured by SMPS for 480 min. The wall losses of particles are size-dependent and, thus, we used a size-dependent particle 265 wall-loss correction approach, which is described in detail in the supplement.

Besides, the following text and Fig. R2 were added in the revised supplement to explain how the size dependent wall loss constant was obtained.

S1. Size-dependent wall loss correction method

270 In the present work, the size-dependent particle wall-loss rate constants were determined based on the SMPS-measured particle size distribution. The first-order loss rate constants (k_i) of particles in each size bin i across all measured sizes were firstly calculated as the slope of the corresponding ln-linear fit line:

$$\ln[M_i(t)] = -k_i t + C \quad (S1)$$

275 where M_i ($\mu\text{g m}^{-3}$) is the mass concentration of particles in size bin i at time t (min) and C is an arbitrary constant. Then, the relationship between the k_i and the particle diameter ($d_{p,i}$) can be described as follows:

$$k_i(d_{p,i}) = ad_{p,i}^b + cd_{p,i}^{-d} \quad (S2)$$

The optimized fitted line shown in Fig. S1 can express well our independent seed experimental results. Parameters a , b , c , and d in Eq. (S2) were determined to be 5.5×10^{-6} , 1.05, 0.18, 1.19, respectively. Therefore, the size-dependent loss rate (k) of 280 ammonium sulfate particles can be expressed as $k = 5.5 \times 10^{-6} \times d_p^{1.05} + 0.18 \times d_p^{-1.19}$.

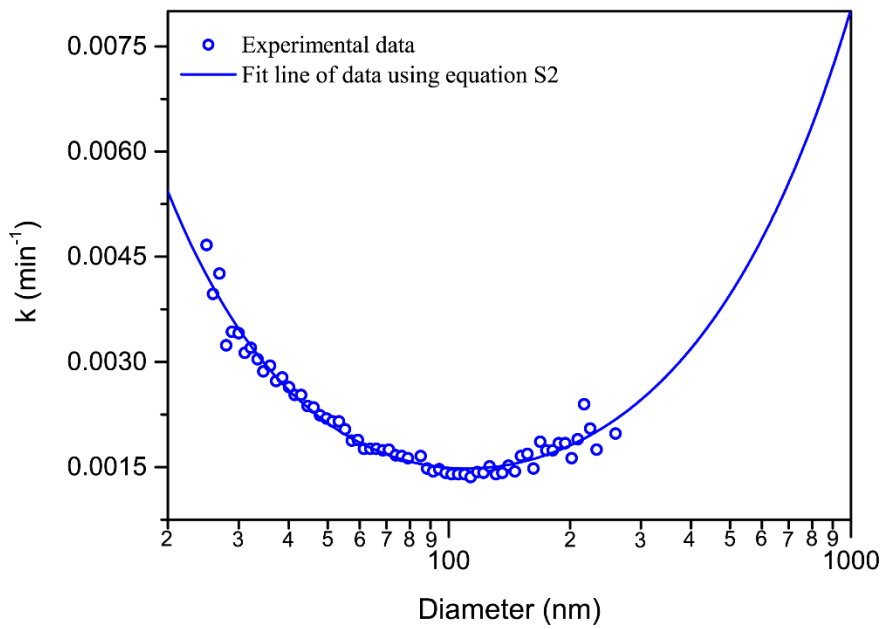
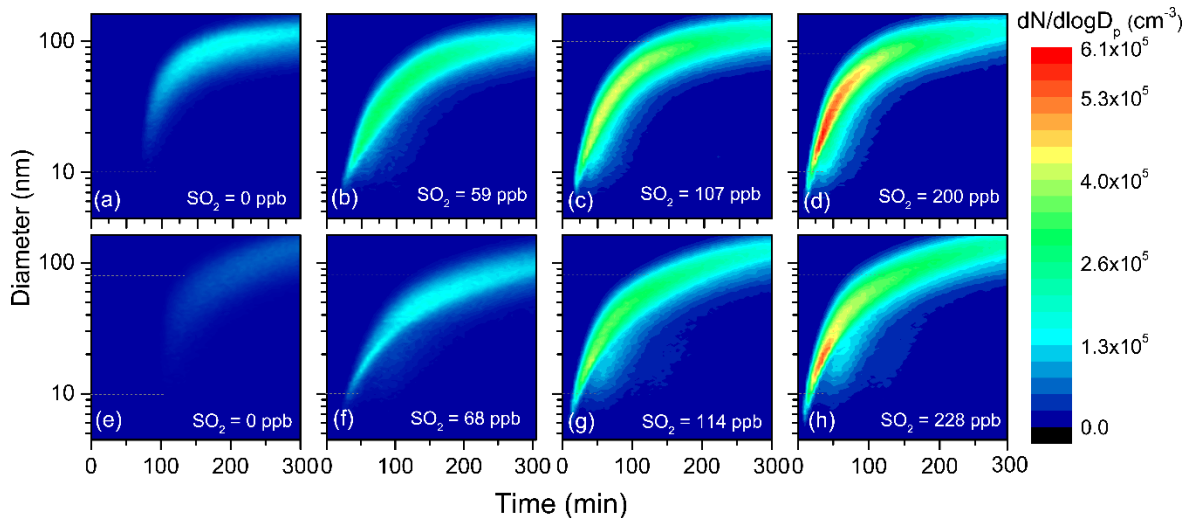


Figure S1. Wall loss rate constant of particles as a function of particle diameter.

Figure 1: It would be better to change the plots all in the same scale for easy comparison of different conditions.
285

Author Reply:

Figure 1 has been revised according to the comment of the Referee as follows:



290 **Figure 1.** Evolutions of the number distributions of aerosol particles generated from TMB photooxidation in low- NO_x (Panels a–d) and high- NO_x (Panels e–h) experiments.

L305: an extra space before “to”

Author Reply:

295 The extra space has been deleted in the revised manuscript.

L367: Please add the recent paper by Chen et al. 2020 also demonstrate that OS-228 could be from isoprene-derived SOA.

Author Reply:

300 We have cited the study of Chen et al. (2020b) and added the related description. Please, refer to the last comment.

L389: The author should also consider adding Zhang et al. 2019 here, which discussed the effects of inorganic sulfates to organosulfates conversion in affecting aerosol growth, 305 multiphase chemistry, and pH.

Author Reply:

The paper by Zhang et al. (2019) has now been cited and the original sentence was modified as follow:

310 **The conversion of inorganic sulfates to organosulfates could cause changes in aerosol growth, multiphase chemistry, and acidity (Zhang et al., 2019; Riva et al., 2019).**

L525: As mentioned, OS-228 was observed by Chen et al. 2020 from the aging of isoprene-SOA. Even though the source might be different from the OS-228 here, the author should mention it in the conclusion instead of defining OS-228 as from unknown 315 source.

Author Reply:

We have carefully read the literature suggested by the Referee. Chen et al. (2020b) investigated the heterogeneous OH oxidation of 2-methyltetrol sulfate diastereomers and identified OS at *m/z* 227 as the oxidation product of 2-methyltetrol sulfate 320 diastereomers. Methyltetrol sulfates are significant tracers for isoprene-derived SOA. Therefore, the OH aging of isoprene SOA is also a potential source of OS-228 in the

atmosphere. The inappropriate conclusion has been removed in the revised manuscript. We have added the following text in Sect. 3.1.3 to describe the findings in the study by Chen et al. (2020b).

325 Page 18, lines 507–512

More recently, Chen et al. (2020b) suggested that heterogeneous OH oxidation of isoprene-derived SOA can contribute to the formation of an organosulfate with molecular weight at 228. Our results show the detection of OS-226, OS-228, OS-240, and OS-268 organosulfates, which are isomers of organosulfates derived from isoprene
330 (Cai et al., 2020), isoprene (Chen et al., 2020b), limonene (Cai et al., 2020), and limonene (Boris et al., 2016), respectively.

References:

335 Chen, Y., et al. (2020). "Heterogeneous Hydroxyl Radical Oxidation of Isoprene-Epoxydiol-Derived Methyltetrol Sulfates: Plausible Formation Mechanisms of Previously Unexplained Organosulfates in Ambient Fine Aerosols." Environmental Science & Technology Letters 7(7): 460-468.

Zhang, Y., et al. (2019). "Joint Impacts of Acidity and Viscosity on the Formation of
340 Secondary Organic Aerosol from Isoprene Epoxydiols (IEPOX) in Phase Separated Particles." ACS Earth and Space Chemistry 3(12): 2646-2658.

References

345 Apsokardu, M. J., and Johnston, M. V.: Nanoparticle growth by particle-phase chemistry, *Atmos. Chem. Phys.*, 18, 1895-1907, 10.5194/acp-18-1895-2018, 2018.

Boris, A. J., Lee, T., Park, T., Choi, J., Seo, S. J., and Collett Jr, J. L.: Fog composition at Baengnyeong Island in the eastern Yellow Sea: detecting markers of aqueous atmospheric oxidations, *Atmos. Chem. Phys.*, 16, 437-453, 10.5194/acp-16-437-2016, 350 2016.

Cai, D., Wang, X., Chen, J., and Li, X.: Molecular characterization of organosulfates in highly polluted atmosphere using ultra-high-resolution mass spectrometry, *J. Geophys. Res.-Atmos.*, 125, 10.1029/2019jd032253, 2020.

Charan, S. M., Buenconsejo, R. S., and Seinfeld, J. H.: Secondary organic aerosol yields from the oxidation of benzyl alcohol, *Atmos. Chem. Phys.*, 20, 13167-13190, 355 10.5194/acp-20-13167-2020, 2020.

Chen, L., Bao, Z., Wu, X., Li, K., Han, L., Zhao, X., Zhang, X., Wang, Z., Azzi, M., and Cen, K.: The effects of humidity and ammonia on the chemical composition of secondary aerosols from toluene/NO_x photo-oxidation, *Sci. Total Environ.*, 728, 360 138671, 10.1016/j.scitotenv.2020.138671, 2020a.

Chen, T., Liu, Y., Ma, Q., Chu, B., Zhang, P., Liu, C., Liu, J., and He, H.: Significant source of secondary aerosol: formation from gasoline evaporative emissions in the presence of SO₂ and NH₃, *Atmos. Chem. Phys.*, 19, 8063-8081, 10.5194/acp-19-8063-2019, 2019.

365 Chen, Y., Zhang, Y., Lambe, A. T., Xu, R., Lei, Z., Olson, N. E., Zhang, Z., Szalkowski, T., Cui, T., Vizuete, W., Gold, A., Turpin, B. J., Ault, A. P., Chan, M. N., and Surratt, J. D.: Heterogeneous Hydroxyl Radical Oxidation of Isoprene-Epoxydiol-Derived Methyltetrol Sulfates: Plausible Formation Mechanisms of Previously Unexplained Organosulfates in Ambient Fine Aerosols, *Environ. Sci. Technol. Lett.*, 7, 460-468, 370 10.1021/acs.estlett.0c00276, 2020b.

Chu, B., Zhang, X., Liu, Y., He, H., Sun, Y., Jiang, J., Li, J., and Hao, J.: Synergetic formation of secondary inorganic and organic aerosol: effect of SO₂ and NH₃ on particle formation and growth, *Atmos. Chem. Phys.*, 16, 14219-14230, 2016.

Han, Y., Gong, Z., Liu, P., de Sá, S. S., McKinney, K. A., and Martin, S. T.: Influence 375 of Particle Surface Area Concentration on the Production of Organic Particulate Matter in a Continuously Mixed Flow Reactor, *Environ. Sci. Technol.*, 53, 4968-4976, 10.1021/acs.est.8b07302, 2019.

Jaoui, M., Edney, E. O., Kleindienst, T. E., Lewandowski, M., Offenberg, J. H., Surratt, J. D., and Seinfeld, J. H.: Formation of secondary organic aerosol from irradiated α -pinene/toluene/NO_xmixtures and the effect of isoprene and sulfur dioxide, *J. Geophys. Res.*, 113, 10.1029/2007jd009426, 2008.

380 Jiang, X., Chen, L., You, B., Liu, Z., Wang, X., and Du, L.: Joint impacts of atmospheric SO₂ and NH₃ on the formation of nanoparticles from photooxidation of a typical biomass burning compound, *Environmental Science: Nano*, 10.1039/d0en00520g, 2020.

385 Kleindienst, T. E., Edney, E. O., Lewandowski, M., Offenberg, J. H., and Jaoui, M.:

Secondary organic carbon and aerosol yields from the irradiations of isoprene and α -pinene in the presence of NO_x and SO_2 , *Environ. Sci. Technol.*, 40, 3807-3812, 10.1021/es052446r, 2006.

390 Liu, C., Chen, T., Liu, Y., Liu, J., He, H., and Zhang, P.: Enhancement of secondary organic aerosol formation and its oxidation state by SO_2 during photooxidation of 2-methoxyphenol, *Atmos. Chem. Phys.*, 19, 2687-2700, 10.5194/acp-19-2687-2019, 2019.

395 Liu, T., Wang, X., Hu, Q., Deng, W., Zhang, Y., Ding, X., Fu, X., Bernard, F., Zhang, Z., Lu, S., He, Q., Bi, X., Chen, J., Sun, Y., Yu, J., Peng, P., Sheng, G., and Fu, J.: Formation of secondary aerosols from gasoline vehicle exhaust when mixing with SO_2 , *Atmos. Chem. Phys.*, 16, 675-689, 10.5194/acp-16-675-2016, 2016.

400 McVay, R. C., Cappa, C. D., and Seinfeld, J. H.: Vapor-Wall Deposition in Chambers: Theoretical Considerations, *Environ. Sci. Technol.*, 48, 10251-10258, 10.1021/es502170j, 2014.

Nah, T., McVay, R. C., Zhang, X., Boyd, C. M., Seinfeld, J. H., and Ng, N. L.: Influence of seed aerosol surface area and oxidation rate on vapor wall deposition and SOA mass yields: a case study with α -pinene ozonolysis, *Atmos. Chem. Phys.*, 16, 9361-9379, 10.5194/acp-16-9361-2016, 2016.

405 Riva, M., Chen, Y., Zhang, Y., Lei, Z., Olson, N. E., Boyer, H. C., Narayan, S., Yee, L. D., Green, H. S., Cui, T., Zhang, Z., Baumann, K., Fort, M., Edgerton, E., Budisulistiorini, S. H., Rose, C. A., Ribeiro, I. O., RL, E. O., Dos Santos, E. O., Machado, C. M. D., Szopa, S., Zhao, Y., Alves, E. G., de Sa, S. S., Hu, W., Knipping, E. M., Shaw, S. L., Duvoisin Junior, S., de Souza, R. A. F., Palm, B. B., Jimenez, J. L., Glasius, M., Goldstein, A. H., Pye, H. O. T., Gold, A., Turpin, B. J., Vizuete, W., Martin, S. T., Thornton, J. A., Dutcher, C. S., Ault, A. P., and Surratt, J. D.: Increasing Isoprene Epoxydiol-to-Inorganic Sulfate Aerosol Ratio Results in Extensive Conversion of Inorganic Sulfate to Organosulfur Forms: Implications for Aerosol Physicochemical Properties, *Environ. Sci. Technol.*, 53, 8682-8694, 10.1021/acs.est.9b01019, 2019.

410 Vivanco, M. G., Santiago, M., Martinez-Tarifa, A., Borras, E., Rodenas, M., Garcia-Diego, C., and Sanchez, M.: SOA formation in a photoreactor from a mixture of organic gases and HONO for different experimental conditions, *Atmos. Environ.*, 45, 708-715, 10.1016/j.atmosenv.2010.09.059, 2011.

415 Wyche, K. P., Monks, P. S., Ellis, A. M., Cordell, R. L., Parker, A. E., Whyte, C., Metzger, A., Dommen, J., Duplissy, J., Prevot, A. S. H., Baltensperger, U., Rickard, A. R., and Wulfert, F.: Gas phase precursors to anthropogenic secondary organic aerosol: detailed observations of 1,3,5-trimethylbenzene photooxidation, *Atmos. Chem. Phys.*, 9, 635-665, 10.5194/acp-9-635-2009, 2009.

420 Ye, J., Abbatt, J. P. D., and Chan, A. W. H.: Novel pathway of SO_2 oxidation in the atmosphere: reactions with monoterpene ozonolysis intermediates and secondary organic aerosol, *Atmos. Chem. Phys.*, 18, 5549-5565, 10.5194/acp-18-5549-2018, 2018.

Zhang, R., Wang, G., Guo, S., Zamora, M. L., Ying, Q., Lin, Y., Wang, W., Hu, M., and Wang, Y.: Formation of urban fine particulate matter, *Chem. Rev.*, 115, 3803-3855, 10.1021/acs.chemrev.5b00067, 2015.

430 Zhang, X., Cappa, C. D., Jathar, S. H., McVay, R. C., Ensber, J. J., Kleeman, M. J., and

Seinfeld, J. H.: Influence of vapor wall loss in laboratory chambers on yields of secondary organic aerosol, *P. Natl. Acad. Sci. USA*, 111, 5802-5807, 2014.

Zhang, Y., Chen, Y., Lei, Z., Olson, N. E., Riva, M., Koss, A. R., Zhang, Z., Gold, A., Jayne, J. T., Worsnop, D. R., Onasch, T. B., Kroll, J. H., Turpin, B. J., Ault, A. P., and Surratt, J. D.: Joint Impacts of Acidity and Viscosity on the Formation of Secondary Organic Aerosol from Isoprene Epoxydiols (IEPOX) in Phase Separated Particles, *ACS Earth Space Chem.*, 3, 2646-2658, 10.1021/acsearthspacechem.9b00209, 2019.

Zhao, D., Schmitt, S. H., Wang, M., Acir, I.-H., Tillmann, R., Tan, Z., Novelli, A., Fuchs, H., Pullinen, I., Wegener, R., Rohrer, F., Wildt, J., Kiendler-Scharr, A., Wahner, A., and Mentel, T. F.: Effects of NO_x and SO_2 on the secondary organic aerosol formation from photooxidation of α -pinene and limonene, *Atmos. Chem. Phys.*, 18, 1611-1628, 10.5194/acp-18-1611-2018, 2018.